Accepted in Journal of Materials Science, 2007
Archived in Dspace@nitrk
http://dspace.nitrkl.ac.in/dspace

Properties of Ni/YSZ Porous Cermets Prepared by Electroless Coating Technique for SOFC Anode Application

Swadesh K Pratihar[1], A. Dassharma[*] and H.S. Maiti[*]
Department of Ceramic Engineering
National Institute of Technology
Rourkela – 769 008 India

Abstract

A conceptual nickel – yttria stabilized zirconia (Ni/YSZ) cermet has been prepared by coating YSZ particles with metallic nickel using electroless coating technique. Concentration of nickel was varied between 5 and 60 volume %. Bulk samples were prepared by uniaxial pressing followed by sintering in the temperature range 1200 – 1350^{o}C with a soaking time of 2-6 h. Thorough investigation on the electrical characteristics, thermal expansion behavior of the samples have been performed as a function of Ni-content in the cermet. Thermal expansion behavior and conductivity measurement results suggest that the samples prepared by this technique are suitable for solid oxide fuel cell (SOFC) anode application at Ni concentration as low as 20 volume %.

Keywords: Electroless coating; Ni/YSZ cermet; Solid oxide fuel cell; Electrical and thermal properties

1. Corresponding author: Tel: 91 661 2462206; Fax: 91 661 247 2926
E-mail: skpratihar@nitrkl.ac.in (S.K. Pratihar)

* Electroceramics Division, Central Glass & Ceramic Research Institute, Kolkata – 700 032, India.

1. Introduction

Solid oxide fuel cells (SOFC) are getting importance as energy conversion systems due to their high efficiency, modularity in design and environmentally friendly nature. The most popular anode material for solid oxide fuel cell (SOFC) is nickel yttria stabilized zirconia (Ni-YSZ) cermet [1-3]. In order to achieve the best performance as anode cermet, three main factors should be considered. First of all, anode should have high electrical conductivity to reduce the ohmic loss. Next, it should have enough electrochemical activity to reduce the activation polarization that is related to the electrochemical reaction at anode. And lastly, it should have proper microstructural condition to reduce the concentration polarization, which is related to the diffusion of the reactants or products of the electrode reaction. These factors are necessary to obtain the best performance of the anode and partial fulfillment of these conditions is not sufficient for the proper operation of SOFC. For example, for higher electrical conductivity, higher Ni content is the best choice but; higher Ni content leads to instability of microstructure due to Ni coarsening and thermal expansion coefficient mismatch. On the other hand, for lower concentration polarization, high porous composite is better but one cannot guarantee the proper mechanical and electrical properties. Open porosity is required for the electrode to supply fuel and for removal of reaction products. The nickel particles forming a percolative network have a large catalytic activity and are responsible for transporting electron from the electrode reaction site to the current collector. The addition of YSZ is necessary to support the nickel particles, to inhibit Ni-coarsening by sintering into larger Ni particles at the usual operating temperature of an SOFC, and to give the cermet a thermal expansion coefficient close to that of other cell components [4-7].

The reported works on Ni/YSZ cermet synthesis [8-10] aims to achieve a uniform and homogeneous distribution between the Ni and YSZ phases in the matrix. However cermet

prepared by these techniques behaves as biphasic composite and shows conductivity percolation at 35-40 volume% Ni. Although, such a high amount of Ni meets the conductivity requirement of SOFC anode along with the porosity requirement (35-40%) for lowering concentration polarization, it results in a material that has highest thermal expansion coefficient amongst all the cell components.

It is well established that the metallic conductivity of Ni/YSZ cermet (above percolation threshold) is achieved by the formation Ni-to Ni chain within the cermet matrix [1-4]. Taking into this fact under consideration, in the present investigation, a conceptual microstructure of the Ni/YSZ has been proposed wherein attempts were made to reduce the thermal expansion coefficient of the cermet anode by lowering the Ni content without compromising its electrical conductivity and porosity. Earlier, we have reported the feasibility of preparing a Ni-coated YSZ cermet following electroless technique [11]. That paper discusses optimization of different process parameters for uniform nickel coating on YSZ surface. We have also reported the effect powder processing routes on the microstructure and properties of Ni/YSZ cermet earlier [12], wherein electrical property of the Ni/YSZ cermets prepared by solid-state, liquid dispersion and electroless coating technique has been correlated with their microstructure. In the present investigation, electrical conductivity and thermal expansion behavior of the samples prepared by electroless technique has been correlated with the microstructure and a systematic study has been made to determine the minimum possible nickel concentration required to have sufficient electrical conductivity for SOFC anode application.

2. Experimental

Ni-YSZ composite powder was prepared using electroless coating technique. In this process the YSZ (8 mol% Y_2O_3 –ZrO_2, TOSOH Corporation, Japan) powder surfaces have been

first sensitized and then catalyzed by Sn-Pd catalyst by dipping the powder in a mixed aqueous solution of stannous chloride ($SnCl_2$) (Qualigens, India) and palladium chloride ($PdCl_2$) (E-mark, India). The sensitization and catalization reactions were carried out in an ultrasonic sensitization bath prior to electroless coating. Metallic nickel was then coated on these surface treated powders by electroless process in an electroless plating bath. Throughout the coating process, the powders were kept suspended within the plating bath by magnetically stirring the bath. The factors, which affected the deposition behavior of nickel, are concentration of palladium chloride in sensitization bath and YSZ particle concentration in sensitization and electroless plating bath. Nickel content of the coated powder was varied from 5-60 volume % in the powder. The coated powders were then pressed in the form of a rectangular bar of dimension 15mm x 3mm x 2mm following conventional pressing. These pressed pellets were sintered in air in the temperature range 1200^{o}C-1300^{o}C for 4h when NiO-YSZ was formed. The air-sintered pellets were then reduced under mixed atmosphere of hydrogen and argon at 1000^{o}C for 2h to convert NiO back to metallic nickel. Porosity of the samples was measured by water displacement method using Archimedes' principle. DC electrical conductivity of the reduced samples were measured by four-probe technique using a 7.5 digit multimeter (HP 3458A). Unfluxed platinum paste was used as contacts for electrical conductivity measurement. For each sample, measurement was carried out at different temperatures in the range from ambient to 1000^{o}C under mixed atmosphere of hydrogen and argon. Thermal expansion of the bulk samples was measured by NETZSCH dilatometer model DIL 402 C. For this, the sintered samples were made in the form of rods having diameter 6mm and length 10mm. The heating rate was maintained at 10^{o}C/min. For all the samples the measurement was carried out from room temperature to 1000^{o}C. The thermal expansion coefficient (TEC) value was calculated from the expansion curve. For

NiO/YSZ composite, the measurement was carried out at air atmosphere, whereas the reduced samples (Ni/YSZ cermets) were measured under argon atmosphere. For microstructural study, a few representative samples were examined under scanning electron microscope (LEICA- S440). Global elemental mapping for Ni and Zr was also performed to find the distribution of Ni and YSZ in the samples.

3. Results and discussion

It is observed that in NiO/YSZ composite porosity changes on reduction in H_2 + Ar atmosphere. The observed change in porosity for 40 vol% Ni/YSZ samples prepared by electroless coating technique is presented in Fig.1. The porosity changes before and after reduction is found to follow a straight-line behavior. Similar results have also been reported in literature [14]. Both NiO and Ni have face centered cubic lattice having lattice parameters 4.1769 A^o and 3.5238 A^o respectively. The density of NiO and Ni are 6.806 gm/cc and 8.907 gm/cc respectively. Hence the reduction of NiO/YSZ composite in reducing atmosphere to form Ni/YSZ cermet is associated with an increase in porosity due to loss of oxygen and crystallographic change. Moreover, lower density of NiO as compared to Ni causes an increase in matrix porosity due to loss of oxygen of NiO during conversion to Ni. This fact should be taken into account for preparation of a cermet with desired and controlled porosity.

Fig.2 represents the SEM fractographs of 40 vol% Ni/YSZ sample. Fig.2a represents the same before reduction and (b) represents that after reduction. It is clear from the micrograph that an increase in porosity of the samples occurs upon reduction. This supports our observation for porosity presented in Fig.1 and could be explained as stated above. However, the two different phases namely NiO or Ni and YSZ are not clearly resolved from the microstructure.

A typical back scattered image of 40 vol% Ni/YSZ cermet along with Zr and Ni global elemental mapping is shown in Fig.3. Formation of a continuous nickel ring around the YSZ particles can be visualized easily for the Fig.3c (Ni mapping). The interlinking of nickel particles around YSZ particle clusters can be seen in Fig.3c. This also indicated the effectiveness of the electroless coating technique used and fulfils the basis objective of the conceptual microstructure adopted in this investigation. Though the Fig.3b (Zr mapping) indicates some large zirconia particles in higher magnification it is seen that these zirconia particles are actually a cluster of nickel coated fine YSZ powder. A combination of the Fig.3b and (c) together will result in Fig.3a. The porous structure can also be seen in Fig.3a.This was possible due to very nature of the preparation technique used in this investigation. Similar microstructure has been reported earlier [12].

Fig.4 shows the thermal expansion behavior of YSZ and NiO/YSZ composites containing 20 and 30 vol% Ni in air at a heating rate of 10^{o}C/min. As expected, percentage thermal expansion increases with temperature for all the samples. The slope for the NiO/YSZ samples also increases with increasing nickel content. Among these three samples the expansion is found to be lowest for the YSZ electrolyte. It may be inferred form this study that addition of nickel in YSZ increases its thermal expansion as the TEC value for YSZ is $10.3x10^{-6}/^{o}$C, whereas it is $14.1x10^{-6}/^{o}$C for NiO [15].

The TEC of a composite material can be predicted from the TEC values of the individual phases using Kerner's model [16]. For composite materials, Kerner proposed that the TEC is expressed by the following equation:

$$\beta_c = \Sigma\, \beta_i V_i + 4\,(G_m/K_c)\,\Sigma((K_c-K_i)/(4G_m + 3K_i))(\beta_m - \beta_i)\, V_i \qquad (1)$$

where, β is the average volume expansion coefficient, K is the bulk modulus, and the subscripts i, c, and m represent elements, mixed composite and matrix respectively. As the differences in bulk and shear moduli between NiO and YSZ are neglected, the second term of the equation becomes negligible. Then the equation (1) can be expressed by linear equation (2) as a function of V_i.

$$\beta_c = \beta_y V_y + \beta_n V_n \quad (2)$$

where the subscripts n and y represent NiO and YSZ respectively. Since the composite in this study is an isotropic material, the instantaneous volume expansion coefficient β_I is described as a TEC by the following equation:

$$\beta_I = 3\alpha_I \quad (3)$$

where α_I is the instantaneous linear thermal expansion. The same is not strictly true; however, for the average linear thermal expansion coefficients calculation the following formula [17] has been used:

$$\beta = 3\alpha\,[1 + (T_2 - T_1)\,\alpha] \quad (4)$$

where T_1 and T_2 are starting and terminal temperature of an experiment.

Fig. 5 shows the TECs of NiO/YSZ composites from 50 to 1000^{o}C in air in comparison with a Kerner's model. The solid line in Fig.5 is calculated using above equation. The points are the experimental results. It is clear that the experimental results closely match with the calculated one. It has been found that the TEC value for this system is strongly depends on its composition (mainly nickel content). TEC is also found to depend on the porosity of the sample. In the above study the sample porosity has been kept constant at 35% in order to nullify the porosity effect by varying the sintering conditions. Samples of constant porosity have been prepared by controlling sintering schedule.

Fig. 6 shows the thermal expansion of Ni/YSZ samples containing 20 and 30 vol% Ni in Ar atmosphere at a heating rate of 10^{o}C/min. The samples were initially sintered in air at high temperature and then reduced under H_2 + Ar atmosphere at 1000^{o}C/2h. For comparison the thermal expansion behavior of YSZ is also included in this figure. The thermal expansion behavior of the Ni/YSZ cermet is found to vary linearly with temperature. As expected the slope of the expansion curve also increases with increasing Ni content in the cermet. The thermal expansion is always higher than that YSZ at all temperatures.

Fig.7 shows the TECs of the cermets from 50 to 1000^{o}C in an inert (Ar) atmosphere with the solid curve calculated using Kerner's model. For calculation of the theoretical TEC value different parameters were taken from Mori et al. [18].

Generally, bulk moduli of a composite material can be calculated. The Ni/YSZ cermet may be considered a particulate composite. Bulk moduli of a composite material are given the by equation [19].

$$\ln K_c = V_n \ln K_n + (1-V_n) \ln K_y \qquad (5)$$

where subscripts c, n and y are for composite, nickel and YSZ respectively. V represents the volume fraction. It is also known that mechanical properties are affected by porosity of the materials. Generally, a relationship between Young's modulus, bulk modulus and shear modulus is expressed by the following equation:

$$E = 9\,KG/(3K+G) \qquad (6)$$

The effect of porosity on young's modulus is expressed by Sprigg's equation (20):

$$E = E_o \exp(-bP) \qquad (7)$$

where E is the Young's modulus with porosity P, b is a constant, and E_0 Young's modulus without any porosity.

These results are consistent with the TECs observed. Thus it is shown that the TEC change can be explained by the relationship between mechanical properties of Ni and YSZ.

The temperature dependent dc electrical conductivity of the samples containing 10 and 20 vol% Ni is represented in Fig.8. It can be seen that the conductivity of the cermet prepared with 10 vol% Ni is low and it increases with temperature, whereas that containing 20 vol% Ni is relatively high and decreases with increase of temperature. The conductivity of the samples containing 10 vol% Ni is 1.84×10^{-4} S/cm at 400^{o}C and 0.25 S/cm at 1000^{o}C. On the other hand the conductivity of the samples containing 20 vol% Ni is 215 S/cm at 400^{o}C and 126 S/cm at 1000^{o}C. The conductivity-temperature data for samples containing 10 vol% Ni are best fitted with an exponential relationship and that containing 20 vol% Ni are best fitted with a linear equation (solid lines in Fig.8). The exponential increase in conductivity in the samples containing 10 vol% Ni is dominated by an activated process similar to that of YSZ [21]. On the other hand the linear decrease in conductivity with temperature is indicative of metallic conduction for samples containing 20 vol% Ni.

The temperature dependent electrical conductivity of the cermets (containing 20-60 vol% nickel and sintered at 1300^{o}C for 4 hours) is represented in Fig.9. The conductivity measured at 1000^{o}C varies in the range 542 – 3048 S/cm for the for nickel contents of 20-60 vol%. For all these cases, the conductivity decreases with increasing temperature showing metallic behavior. As expected the conductivity of these samples, increases with increasing nickel content. Most interesting feature is that the change over from non-metallic to metallic behavior takes place only at 20 vol% Ni which is much lower than the value of 30 vol% nickel normally reported in literature for the samples prepared by other techniques [8-10, 22]. The slope calculated from the linear temperature dependence of conductivity is found lowest for 20 vol% Ni and increases

gradually with Ni content. The lower value of the slope at low volume percent Ni sample is expected by the hindrance effect of porosity and the presence of second phase inclusion (YSZ in this case) on electrical conductivity. As the Ni content in the sample increases the effect of the second phase inclusion (YSZ) decreases from the increase in coating thickness, resulted an in increase in the slope.

The electrical conductivity of the samples containing 5-60 vol% nickel and measured at 1000^{o}C is plotted in Fig.10 as a function of nickel concentration and porosity. A series of S-shaped curves are obtained where each curve correspond to different matrix porosity of the samples. The different matrix porosity of the samples was obtained by varying the sintering conditions of the samples in the temperature range 1200-1350^{o}C for 2-6h. All these plots exhibit a sharp increase in conductivity at around 20 vol% nickel, corresponding to the electrical continuity/discontinuity transition point of the dispersed nickel phase. This is in comparison to the literature value of 30 vol% [8-10, 22]. This variation apparently looks similar to that of biphasic composite system, which cold be explained by percolation theory or effective media theory. However, in this case the system does not behave as a biphasic system due to the very nature of the synthesis technique used. In this method, the YSZ powder surface is coated by metallic nickel following electroless technique. In this case this conductivity transition may be attributed with the nickel coating thickness on YSZ particles. The sharp change in conductivity can be explained from the point of view of attainment of a reasonable coating thickness with increase in Ni content on the YSZ surface, which can impart the metallic behavior in the sample. The conductivity transition at 20 vol% Ni is due to the complete coverage of YSZ surfaces by metallic nickel. With increase in Ni content, the conduction path cross sectional area (nickel coating thickness) increases. This leads to an increase in conductivity of the samples with Ni

content. The conductivity was found to increase with matrix density for all the compositions. This may be attributed with the better Ni-to-Ni contact, which increases with decrease in porosity of the samples, which is very much expected.

The high conductivity at 20 vol% Ni due to complete coverage of YSZ particle by metallic Ni layer synthesized by this technique and the lowest thermal expansion coefficient are the major achievements of this present work. These indicate that materials will have a potential in SOFC anode application. However, the suitability of this material for SOFC application can not be guaranteed until electrochemical performance and the stability of the anode is studied in detail. Further work is necessary demonstrate their effectiveness as SOFC anodes.

4. Conclusions

Samples prepared by this technique show metallic behavior as low as 20 vol% Ni in comparison with that those reported earlier. The TEC value of the samples showing metallic conduction is found lower than the reported one. TEC and electrical conductivity measurement data suggests that samples prepared by this technique will have adequate electrical conductivity and lower thermal expansion mismatch with the other fuel cell components (particularly YSZ electrolyte) when used as anode. Ni and Zr distribution as observed by SEM back scattered mode indicates Ni ring formation around the YSZ particles, which confirms the Ni coating on YSZ powder.

References

[1] N.Q. Minh, J. Am. Ceram. Soc. 76 (1993) 563.

[2] S.P.S. Badwal and K. Foger, Ceramic International 22 (1996) 257.

[3] N.Q. Minh and T. Takahashi, Science and Technology of Ceramic Fuel Cells, Elsevier, New York, 1995.

[4] D.E. Dees, T.D. Claar, T.E. Easler, D.C. Fee and F.C. Mrazek, J. Electrochemical Soc. 134 (1987) 2141.

[5] J. Mizusaki, S. Tsuchiya, K. Waragai, H. Tagawa, A. Yoshihidi and Y. Kuwayama, J. Am. Ceram. Soc. 79 (1996) 109.

[6] G. Maggio, I. Ielo, V. Antonucci and N. Giordano, in : F. Grosz, P. Zegers, S.C. Singhal and O. Yamamoto (Eds.), Solid Oxide Fuel Cells II, The Commission of the European Communities, Luxembourg, 1991, pp. 611- 620.

[7] G.E. Pike and C.H. Seager, J. Appl. Phys. 48 (1997) 5152.

[8] M. Marinsek, K. Zupan and J. Macek, J. Power Sources 86 (2000) 383.

[9] Y. Li, Y. Xie, J. Gong, Y. Chen and Z. Zhang, Mat. Sci. Engg. B 86 (2001) 119.

[10] S.T. Aruna, M. Muthuraman and K.C. Patil, Solid State Ionics 111 (1998) 45.

[11] Swadesh K. Pratihar, A. Das Sharma, R.N. Basu and H.S. Maiti, Journal of Power Sources 129 (2004)138.

[12] Swadesh K Pratihar, A. Das Sharma and H.S. Maiti, Mat. Res. Bull., 40 (2005) 1936.

[13] S.K. Pratihar, R.N. Basu, A. Das Sharma and H.S. Maiti, Indian Patent, No. 306 / DEL / 01 dated. 19.03.01.

[14] M. Radovic and E. Lara-Curzio, Acta. Mat. 52 (2004) 5747.

[15] H. Takagi, S. Kobayashi, A. Shiratori, K. Nishida, and Y. Sakabe, in Proceedings of 2nd International symposium on SOFCs, F. Grosz, P. Zegers, S.C. Singhal and O. Yamamoto, editors, pp 99, Commission of the European Communities (1991).

[16] E.H. Kerner, Proc. Phys. Soc. London, Ser. B, 69 (1956) 808.

[17] A. Ringuede, J.A. Labrincha and J.R. Frade, Solid State Ionics 141–142 (2001) 549.

[18] M. Mori, T. Yamamoto, H. Itoh, H. Inaba, and H. Tagawa, J. Electrochem. Soc., 145 (1998) 1374.

[19] Y. Kagawa and H. Hatta, Tailoring Ceramic Composites, Agune-Shofu-sha, Tokyo (1990).

[20] R.M. Spriggs, J. Am. Ceram. Soc., 44 (1961) 628.

[21] A. Banerji, P.K. Rohatgi, and W. Reif, Metall, 38 (1984) 656.

[22] K. Okumura, Y. Yamamoto, T. Fuki, S. Hanyu, Y. Kubo, Y. Esaki, M. Hattori, A. Kusunoki, and S. Takeuchi, in Proceedings of the Third International Symposium on Solid Oxide Fuel Cells, S.C. Singhal and H. Iwahara (eds.) Electrochemical Society, Pennington, NJ, 1993, p. 444.

List of Figures

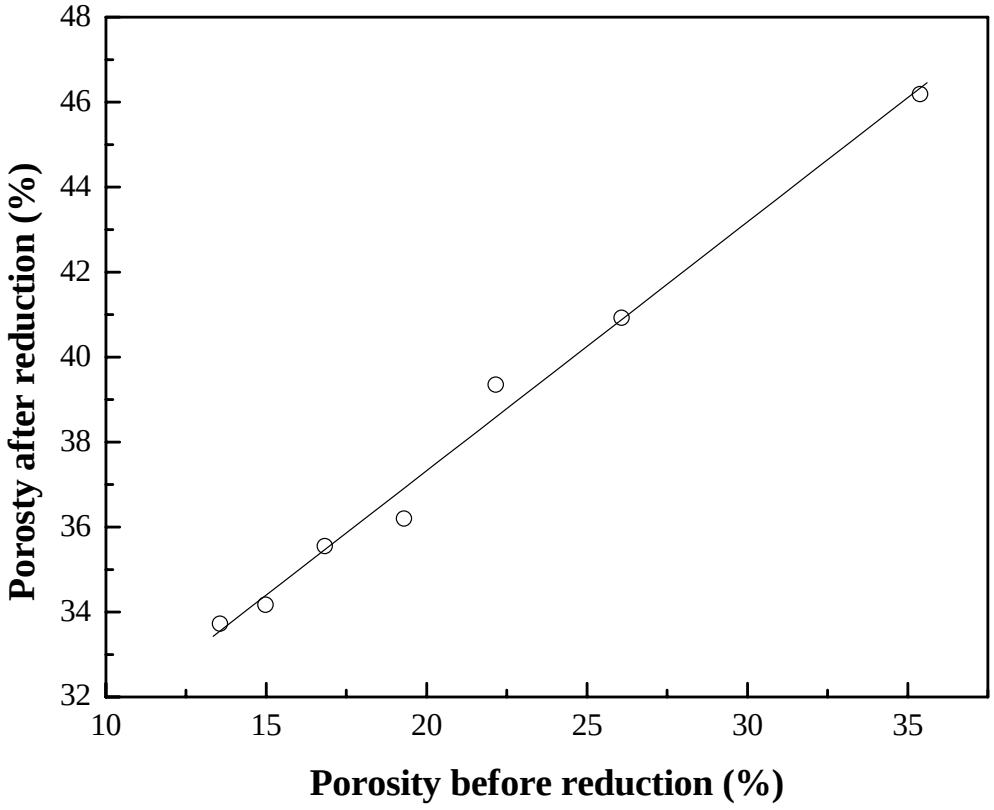

Fig.1 S.K. Pratihar et.al.

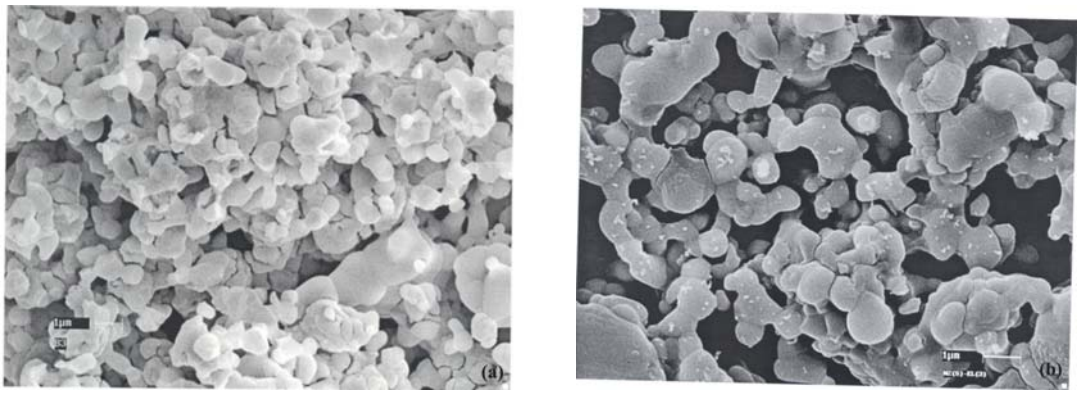

Fig.2 S.K. Pratihar et. al.

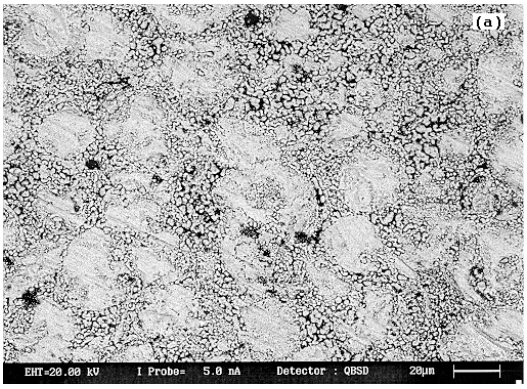

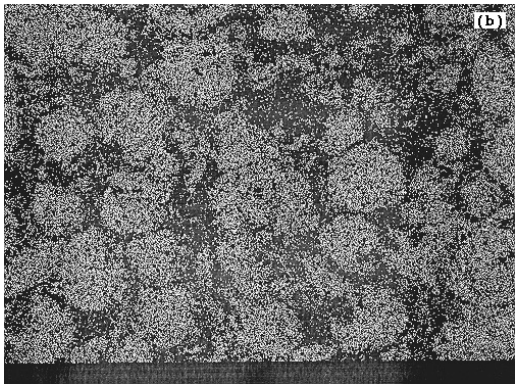

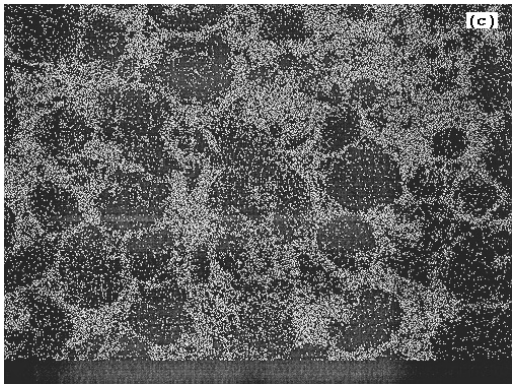

Fig.3 S.K. Pratihar et. al.

.

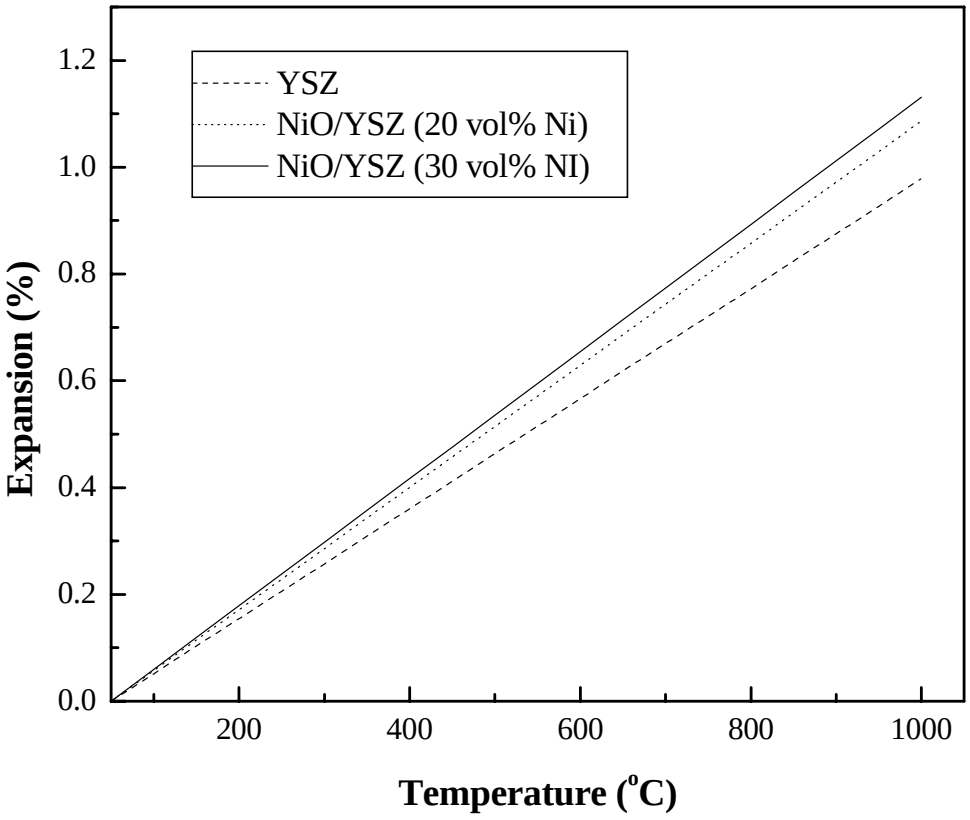

Fig.4 S.K. Pratihar et. al.

.

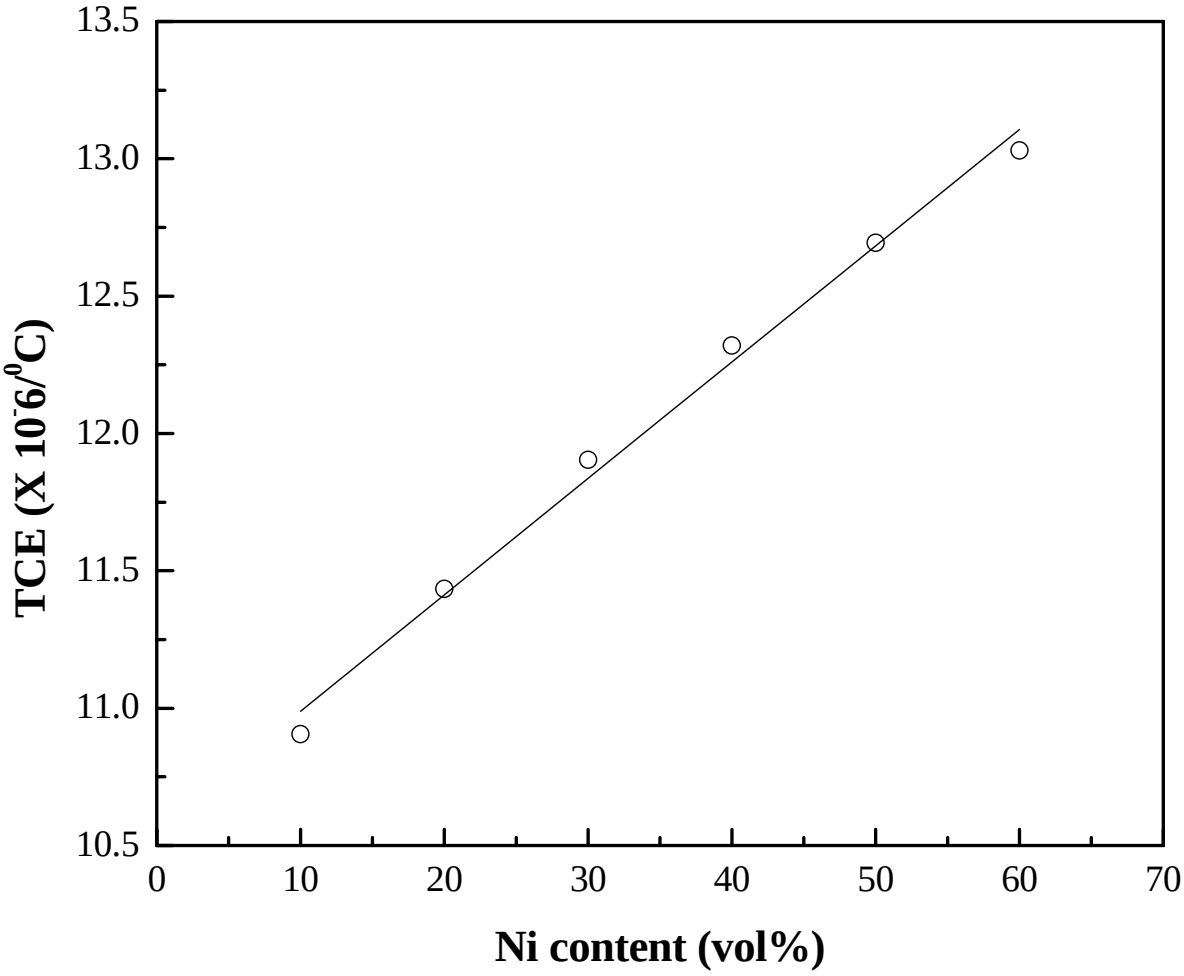

Fig.5 S.K. Pratihar et. al.

.

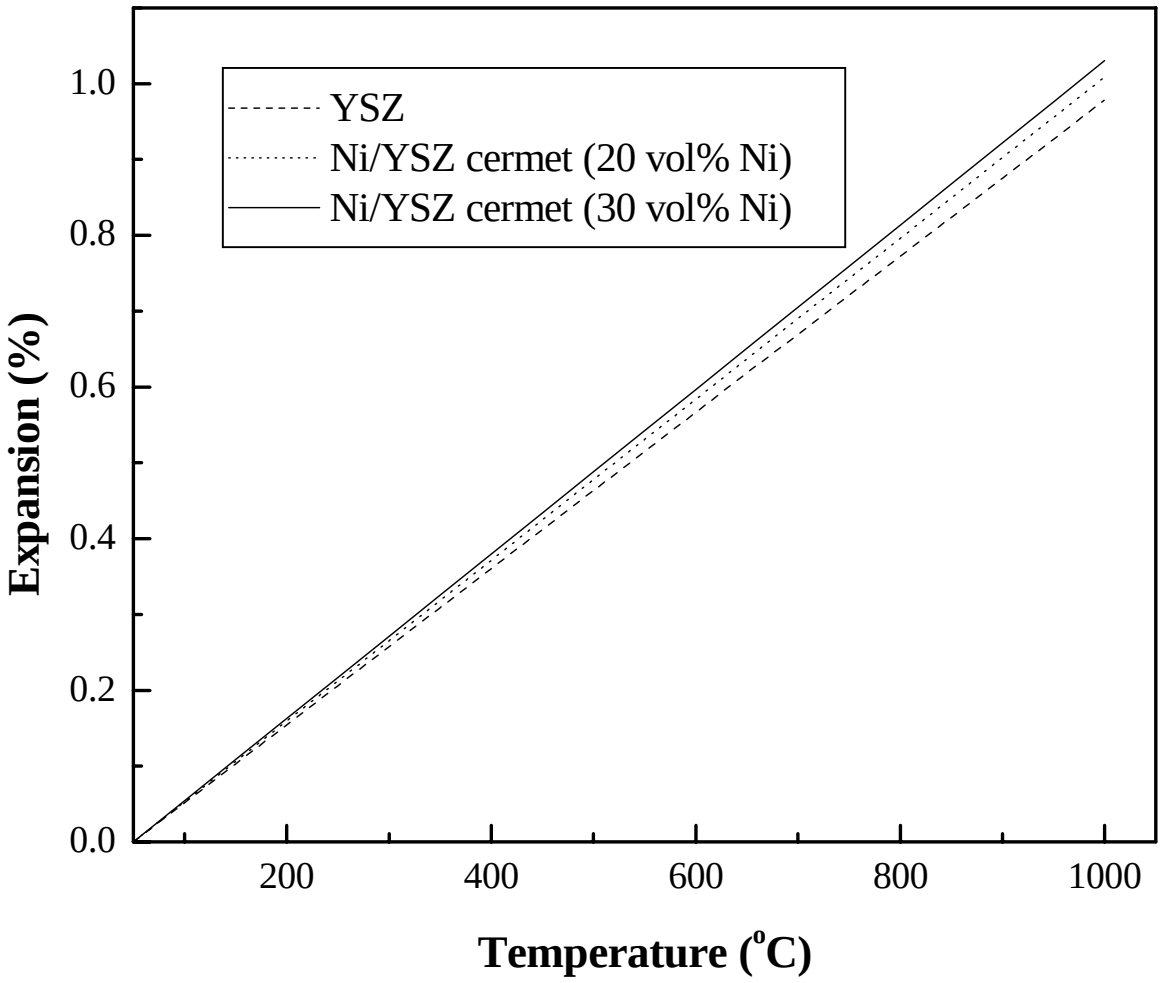

Fig.6 S.K. Pratihar et. al.

.

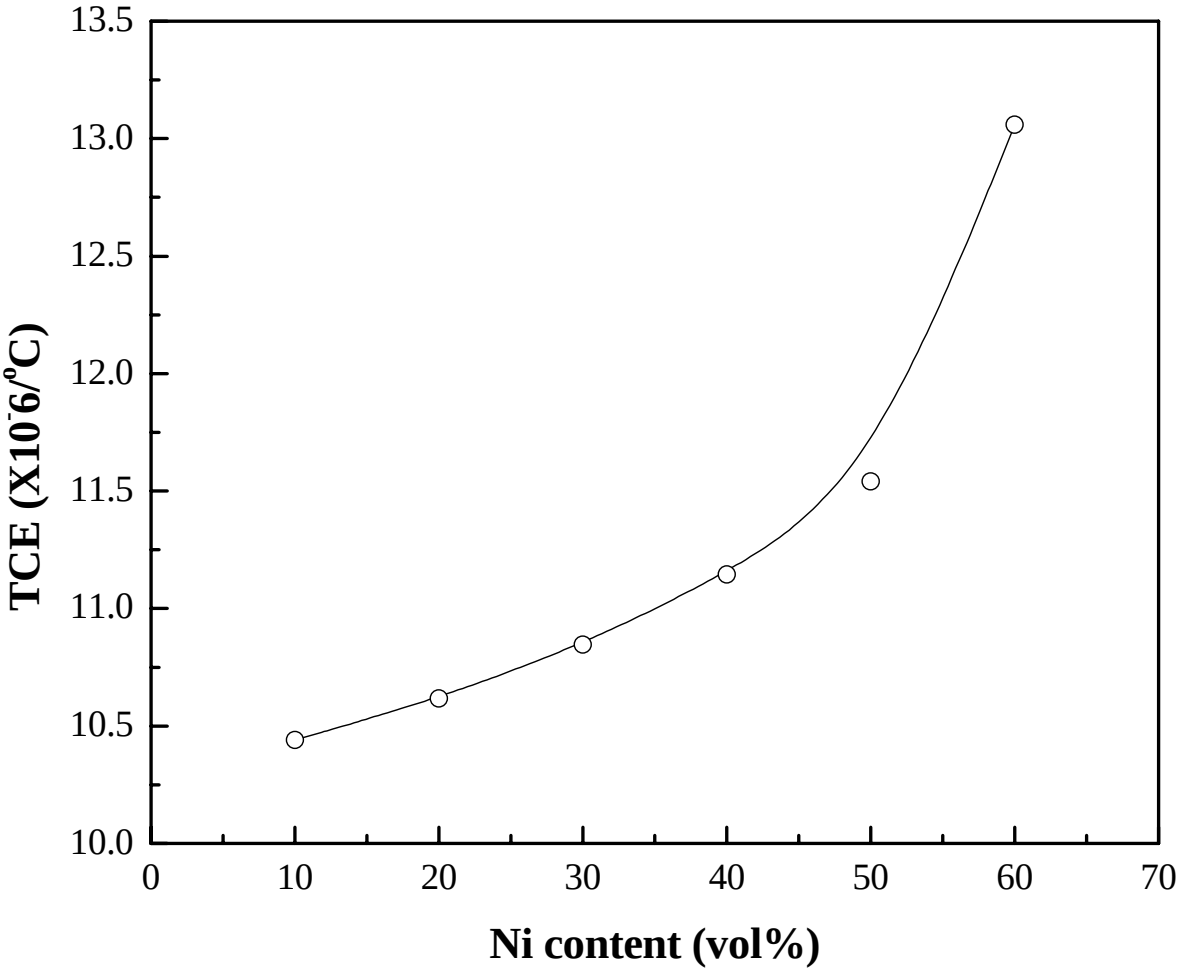

Fig.7 S.K. Pratihar et. al.

.

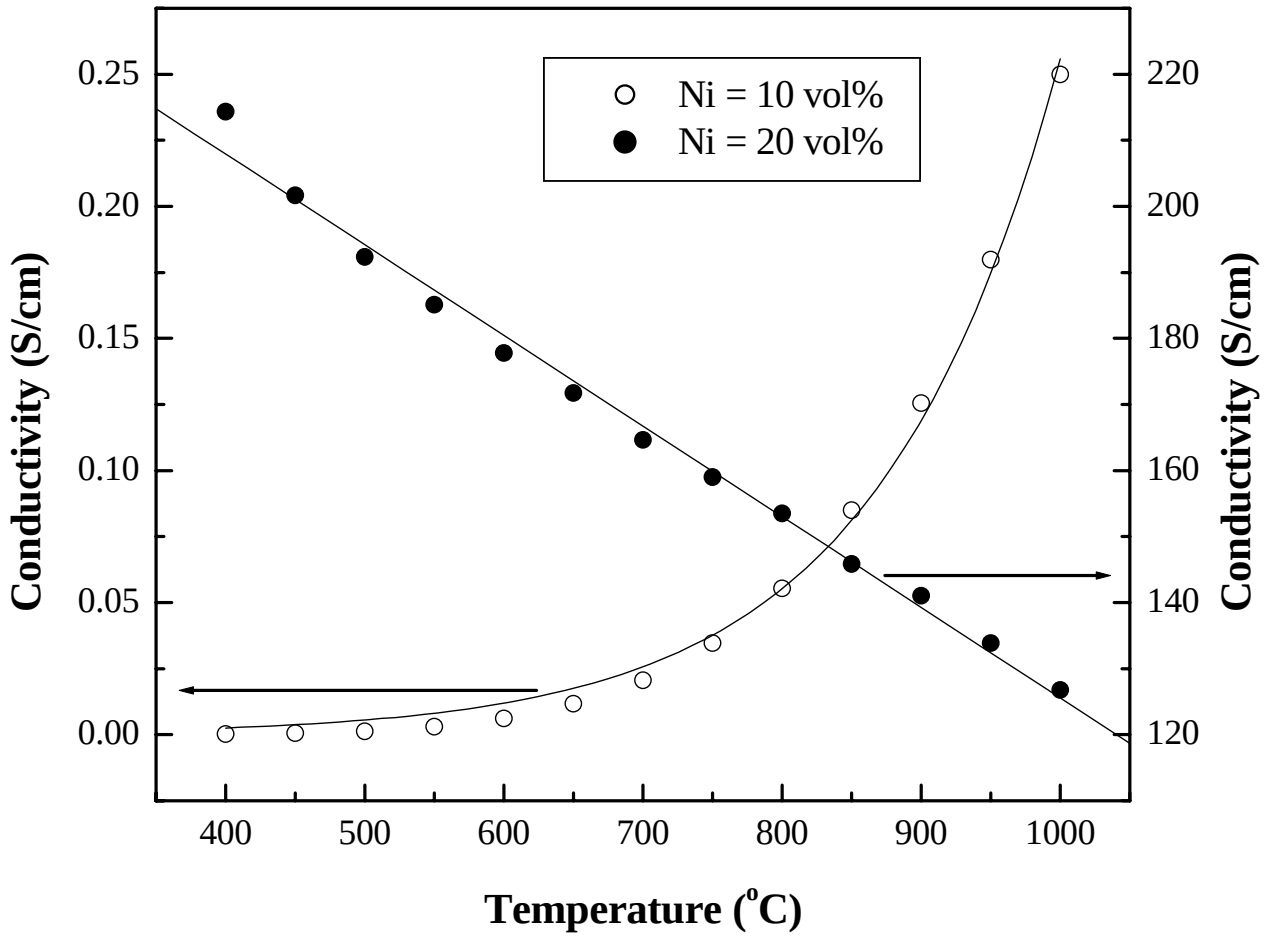

Fig.8 S.K. Pratihar et. al.

.

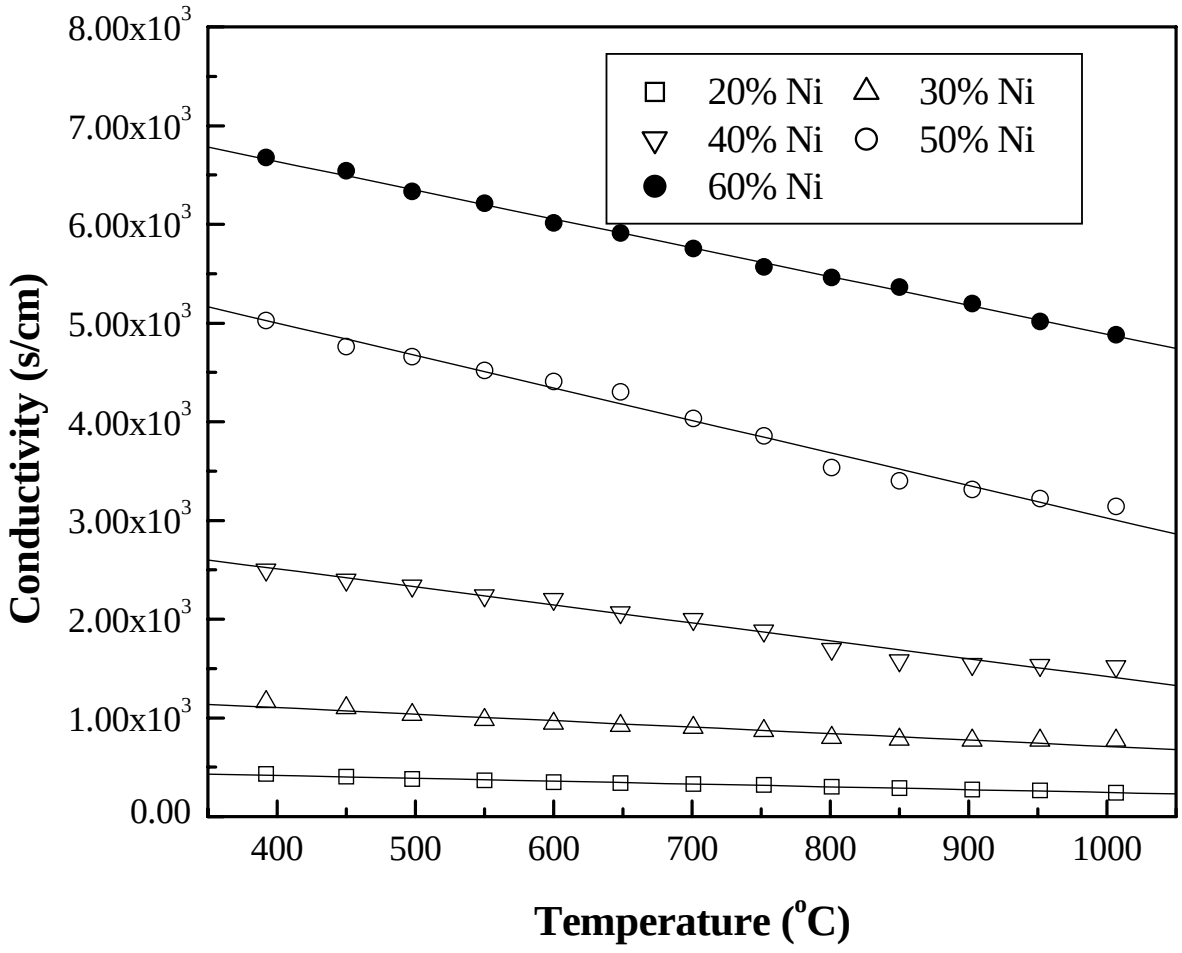

Fig.9 S.K. Pratihar et. al.

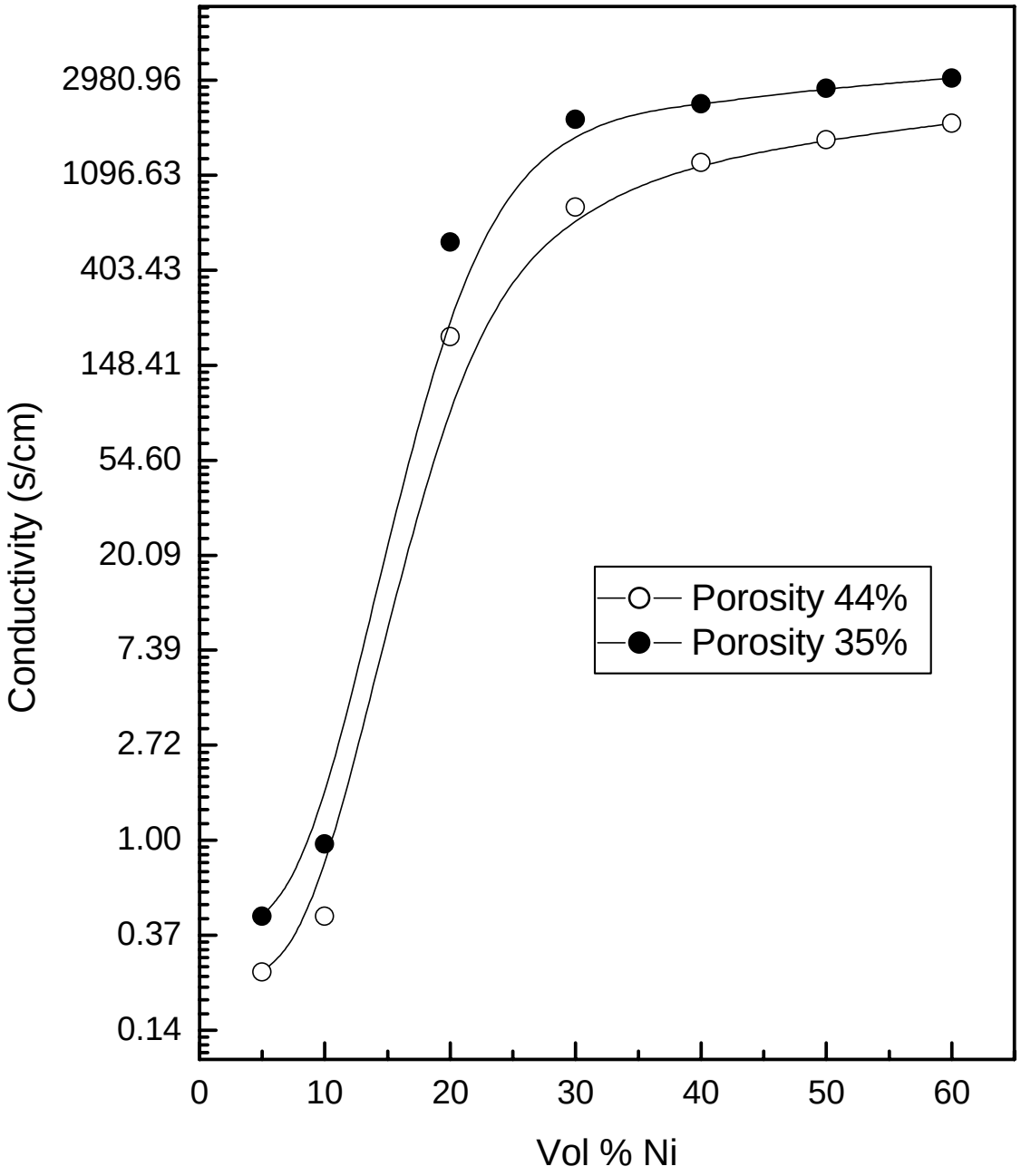

.

Fig.10 S.K. Pratihar et. al.